Inorg. Chem. **2007**, *46*, 10065–10070

Effects of Protonation and Metal Coordination on Intramolecular Charge Transfer of Tetrathiafulvalene Compound

Qin-Yu Zhu,[†] Yu Liu,[†] Wen Lu,[†] Yong Zhang,[†] Guo-Qing Bian,[†] Gai-Yan Niu,[†] and Jie Dai*[,†,‡]

Department of Chemistry & Key Laboratory of Organic Synthesis of Jiangsu Province, Suzhou University, Suzhou 215123, P.R. China and State Key Laboratory of Coordination Chemistry, Nanjing University, Nanjing 210093, P.R. China

Received April 8, 2007

A protonated bifunctional pyridine-based tetrathiafulvalene (TTF) derivative (DMT–TTF–pyH)NO_3 and a copper(II) complex $Cu(acac)_2$(DMT–TTF–py)$_2$ have been obtained and studied. Electronic spectra of the protonated compound show a large ICT (intramolecular charge transfer) band shift ($\Delta\lambda = 136$ nm) compared with that of the neutral compound. Cyclic voltammetry also shows a large shift of the redox potentials ($\Delta E_{1/2}(1) = 77$ mV). Theoretical calculation suggests that the pyridium substituent is a strong π-electron acceptor. Crystal structures of the protonated compound and the metal complex have been obtained. The dihedral angle between least-squares planes of the pyridyl group and the dithiole ring might reflect the intensity of the ICT effect between the TTF moiety and the pyridyl group. It is also noteworthy that the TTF moiety could be oxidized to TTF^{2+} dication by $Fe(ClO_4)_3 \cdot 6H_2O$ when forming a metal complex, while the protonated TTF derivative can only be oxidized to the $TTF^{\bullet+}$ radical cation by $Fe(ClO_4)_3 \cdot 6H_2O$ even with an excess amount of the Fe(III) salt, which can be used to control the oxidation process to obtain neutral TTF, $TTF^{\bullet+}$ radical cation, or TTF^{2+} dication.

Introduction

The TTF moiety is an excellent electron donor and can be oxidized to the corresponding radical cation and dication species sequentially by organic or inorganic oxidizing reagents. In the past decade, one of the biggest challenges in the tetrathiafulvalene (TTF) field is to prepare new TTF compounds attached with various functional groups.[1] By combining the properties of the substituents, these new bifunctional TTF derivatives exhibit distinct properties and are of interest to both material chemists and supramolecular chemists. Herein are some noteworthy aspects. Although TTF charge-transfer (CT) salts have been studied for more than 30 years, the intriguing potential of single molecular D−A (donor−acceptor) bifunctional TTFs has only recently been developed, which is most frequently manifested in molecular-scale electronic devices and nonlinear optical materials.[2] Much effort has been devoted to synthesizing the TTFs with macrocyclic or other units for applications in redox recognition of cations/anions and supramolecular response.[1d,3] Recently, bifunctional molecules featuring one TTF unit and one or two organic fluorescent moieties have been explored, and a series of new redox fluorescent switches has been demonstrated based on the photoinduced electron transfer between the TTF unit and the excited fluorescent unit.[4] More generally, in the field of coordination chemistry, bifunctional

* To whom correspondence should be addressed. Fax: +86 (0)512 65880089. E-mail: daijie@suda.edu.cn.
† Suzhou University.
‡ Nanjing University.

(1) (a) Segura, J. L.; Martin, N. *Angew. Chem., Int. Ed.* **2001**, *40*, 1372−1409. (b) Kobayashi, A.; Fujiwara, E.; Kobayashi, H. *Chem. Rev.* **2004**, *104*, 5243−5264. (c) Derf, F. L.; Mazari, M.; Mercier, N.; Levillain, E.; Trippé, G.; Riou, A.; Richomme, P.; Becher, J.; Garín, J.; Orduna, J.; Gallego-Planas, N.; Gorgues, A.; Sallé, M. *Chem. Eur. J.* **2001**, *7*, 447−455. (d) Nielsen, M. B.; Lomholt, C.; Becher, J. *Chem. Soc. Rev.* **2000**, *29*, 153−227.

(2) (a) Bryce, M. R. *Adv. Mater.* **1999**, *11*, 11−23 and references therein. (b) Andreu, R.; Malfant, I.; Lacroix, P. G.; Cassoux, P. *Eur. J. Org. Chem.* **2000**, 737−741. (c) Herranz, M. A.; Martin, N.; Sanchez, L.; Garin, J.; Orduna, J.; Alcal, R.; Villacampa, B.; Sanchez, C. *Tetrahedron* **1998**, *54*, 11651−11658. (d) Jia, C.; Liu, S.-X.; Tanner, C.; Leiggener, C.; Neels, A.; Sanguinet, L.; Levillain, E.; Leutwyler, S.; Hauser, A.; Decurtins, S. *Chem. Eur. J.* **2007**, 3804−3812. (e) Bryce, M. R.; Green, A.; Moore, A. J.; Perepichka, D. F.; Batsanov, A. S.; Howard, J. A. K.; Ledoux-Rak, I.; González, M.; Martín, N.; Segura, J. L.; Garín, J.; Orduna, J.; Alcalá, R.; Villacampa, B. *Eur. J. Org. Chem.* **2001**, 1927−1935. (f) Tsiperman, E.; Becker, J. Y.; Khodorkovsky, V.; Shames, A.; Shapiro, L. *Angew. Chem., Int. Ed.* **2005**, *44*, 4015−4018.

(3) (a) Jørgensen, T.; Hansen, T. K.; Becher, J. *Chem. Soc. Rev.* **1994**, 41−51. (b) Trippé, G.; Levillain, E.; Derf, F. L.; Gorgues, A.; Sallé, M.; Jeppesen, J. O.; Nielsen, K.; Becher, J. *Org. Lett.* **2002**, *4*, 2461−2464. (c) Liu, S. G.; Liu, H.; Bandyopadhyay, K.; Gao, Z.; Echegoyen, L. *J. Org. Chem.* **2000**, *65*, 3292−3298.

10.1021/ic700672e CCC: $37.00
Published on Web 10/31/2007

TTF derivatives are designed and synthesized by bringing in a coordination moiety that can act as a director of molecular packing, a magnetic d-electron center coupled with π electrons, etc. For example, a TTF-acac derivative has been used to prepare metal complexes that showed intramolecular interactions between the two TTF cores.[5]

Among these bifunctional TTF derivatives, a good established series is pyridine-based TTF derivatives (TTF−py), including nonconjugated and conjugated TTF−py compounds (the TTF moiety and the py group are linked by a σ spacer[6] or a π spacer[2b,7]). Some neutral monocomponent compounds assembled by hydrogen bond or metal coordination bond, some charge-transfer salts with magnetic coupling between TTF radicals and d electrons, and some unique intramolecular charge-transfer (ICT) systems were investigated.[6,7] Recently, a kind of new TTF−py compound has been reported in which the pyridyl group is directly attached to the TTF moiety without a spacer.[8] This type of compound would lead to an increase in the coupling between the π electrons of the TTF moiety and the substituent. However, the intramolecular charge transfer (between the TTF unit and the pyridyl moiety) and redox behavior of this type compound have not been discussed yet. Herein we report two new protonated and metal-coordinated compounds in which the TTF unit is directly linked to the pyridyl group without any spacer. The protonated compound is a strong intramolecular D−A system. Taking advantage of the good coordination ability of the py unit, the D−A properties of the compound can be adjusted by adding the guest ions, which have been demonstrated by theoretical calculation, spectra, and electrochemical measurements. Figure 1 gives the optimized geometries of compound **1**, 2,3-dimethylthio-6-pyridyl-tetrathiafulvalene (DMT−TTF−py), and its protonated cation **2**.

Experimental Section

General Remarks. Elemental analyses of C, H, and N were performed using an EA 1110 elemental analyzer. IR spectra were recorded as KBr pellets on a Nicolet Magna 550 FT-IR spectrometer. UV−vis spectra were recorded in the liquid state on a Shimadzu UV-3150 spectrometer. Cyclic voltammetry (CV) experiments were performed on a CHI600 electrochemistry workstation in a three-electrode system, a single-compartment cell equipped with a platinum working electrode, a platinum wire counter electrode, and a saturated calomel electrode (SCE) as reference. Theoretical calculations were carried out using the GAUSSIAN 03 program package.[9] The molecular structures were fully optimized using the B3LYP functional set and 6-31G basis set. The bifunctional compound DMT−TTF−py was synthesized by a coupling reaction from precursors 4-(4′-pyridyl)-1,3-dithiole-2-one and 4,5-dimethylthio-1,3-dithiole-2-one. This method is based on the strategy described by Becker and Khodorkovsky with some improvements.[8c,10]

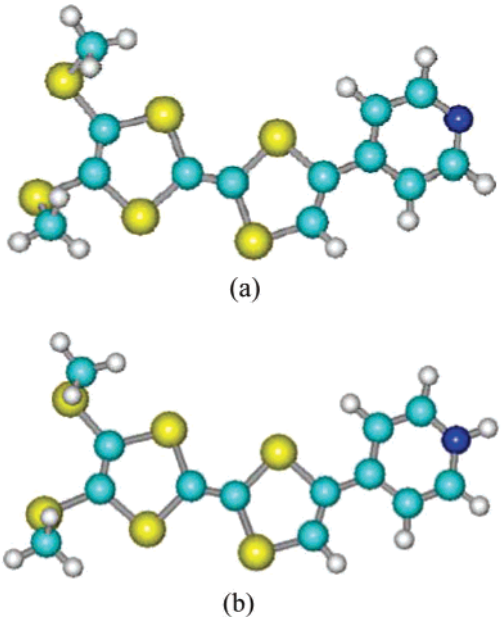

Figure 1. Calculated structure of the compound **1**, DMT−TTF−py (a), and its protonated cation **2** (b) (N, dark blue; S, yellow; C, blue; H, gray).

Synthesis of Compounds. (DMT−TTF−pyH)NO_3 (2). To a solution of DMT−TTF−py (7.5 mg, 0.02 mmol) in dichloromethane (2 mL) was added a solution of $Cu(NO_3)_2$ (4.8 mg, 0.02 mmol) in methanol (2 mL). Then acetylacetone (2 drops) was added to the mixture, forming a dark-purple solution. The final mixture was stirred for 30 min at room temperature and filtered. The purple single crystals were obtained from the filtrate by slow evaporation of the solvent (1.7 mg, yield 20%). Anal. Calcd for $C_{13}H_{12}N_2S_6O_3$: C, 35.76; H, 2.77; N, 6.42. Found: C, 35.22; H, 2.68; N, 5.93. Important IR data: 1627(vs), 1520(vs), 1390(vs), 1304(vs), 812(m), and 776(m) cm^{-1}.

$Cu(acac)_2$(DMT−TTF−py)$_2$ (3). To a solution of DMT−TTF−py (7.5 mg, 0.02 mmol) in dichloromethane (2 mL) was added a solution of $Cu(OAc)_2$ (1.8 mg, 0.01 mmol) in methanol (2 mL). Then acetylacetone (2 drops) was added to the mixture. The final clear solution mixture was stirred for 2 h at room temperature and filtered. The red single crystals were obtained from the filtrate by slow evaporation of the solvent (2.5 mg, yield 25%). Anal. Calcd for $C_{36}H_{38}N_2S_{12}O_4Cu$: C, 42.77; H, 3.79; N, 2.77. Found: C, 42.86; H, 3.58; N, 2.80. Important IR data: 1582(vs), 1520(vs), 1405(vs), 1273(m), 1018(m), 939(m), 794(m), and 771(m) cm^{-1}.

(4) (a) Zhang, G. X.; Zhang, D. Q.; Guo, X. F.; Zhu, D. B. *Org. Lett.* **2004**, *6*, 1209−1212. (b) Giffard, M.; Mabon, G.; Leclair, E.; Mercier, N.; Allain, M.; Gorgues, A.; Molinie, P.; Neilands, O.; Krief, P.; Khodorkovsky, V. *J. Am. Chem. Soc.* **2001**, *123*, 3852−3853. (c) Wang, C.; Zhang, D. Q.; Zhu, D. B. *J. Am. Chem. Soc.* **2005**, *127*, 16372−16373. (d) Zhou, Y.; Zhang, D.; Zhu, L.; Shuai, Z.; Zhu, D. *J. Org. Chem.* **2006**, *71*, 2123−2130.

(5) Massue, J.; Bellec, N.; Chopin, S.; Levillain, E.; Roisnel, T.; Clerac, R.; Lorcy, D. *Inorg. Chem.* **2005**, 44, 8740−8748.

(6) (a) Liu, S.-X.; Dolder, S.; Pilkington, M.; Decurtins, S. *J. Org. Chem.* **2002**, *67*, 3160−3162. (b) Devic, T.; Avarvari, N.; Batail, P. *Chem. Eur. J.* **2004**, *10*, 3697−3707. (c) Jia, C.; Liu, S.-X.; Ambrus, C.; Neels, A.; Labat, G.; Decurtins, S. *Inorg. Chem.* **2006**, *45*, 3152−3154. (d) Jia, C. Y.; Zhang, D. Q.; Xu, Y.; Zhu, D. B. *Synth. Met.* **2003**, *137*, 979−980. (e) Liu, S.-X.; Dolder, S.; Franz, P.; Neels, A.; Stoeckli-Evans, H.; Decurtins. S. *Inorg. Chem.* **2003**, *42*, 4801−4803.

(7) (a) Ouahab, L.; Iwahori, F.; Golhen, S.; Carlier, R.; Sutter, J.-P. *Synth. Met.* **2003**, *133−134*, 505−507. (b) Setifi, F.; Ouahab, L.; Golhen, S.; Yoshida, Y.; Saito, G. *Inorg. Chem.* **2003**, *42*, 1791−1793. (c) Iwahori, F.; Golhen, S.; Ouahab, L.; Carlier, R.; Sutter, J.-P. *Inorg. Chem.* **2001**, *40*, 6541−6542. (d) Lu, H.; Xu, W.; Zhang, D.; Zhu, D. *Chem. Commun.* **2005**, 4777−4779. (e) Xue, H.; Tang, X.-J.; Wu, L.-Z.; Zhang, L.-P.; Tung, C.-H. *J. Org. Chem.* **2005**, *70*, 9727−9734.

(8) (a) Chahma, M.; Wang, X.; Est, A.; Pilkington, M. *J. Org. Chem.* **2006**, *71*, 2750−2755. (b) Wang, L.; Zhang, B.; Zhang, J. *Inorg. Chem.* **2006**, *45*, 6860−6863. (c) Liu, Y.; Zhu, Q.-Y.; Dai, J.; Zhang, Y.; Bian, G.-Q.; Lu, W. *J. Coord. Chem.* **2007**, *60*, 2319−2326.

(9) (a) *Gaussian 03*, revision C.01; Gaussian, Inc.: Wallingford, CT, 2004. (b) Becke, A. D. *J. Chem. Phys.* **1993**, *98*, 5648 and references therein.

(10) Levi, O. P.-T.; Becker, J. Y.; Ellern, A.; Khodorkovsky, V. *Tetrahedron Lett.* **2001**, *42*, 1571−1573.

Table 1. Crystallographic and Refinement Data for Compounds **2** and **3**

	2	**3**
formula	$C_{13}H_{12}N_2O_3S_6$	$C_{36}H_{36}CuN_2O_4S_{12}$
fw	436.61	1008.93
cryst size (mm)	0.60 × 0.40 × 0.39	0.50 × 0.40 × 0.20
cryst syst	monoclinic	triclinic
space group	$P2_1/n$	$P\bar{1}$
a (Å)	10.4949(10)	8.1736(8)
b (Å)	15.2554(13)	8.4516(8)
c (Å)	11.5722(10)	17.625(2)
α (deg)	90.00	82.157(8)
β (deg)	108.427(2)	80.352(8)
γ (deg)	90.00	66.401(6)
V (Å^3)	1757.8(3)	1096.7(2)
Z	4	1
F(000)	896	519
no. of unique reflns	3218	3977
no. of reflns [$I > 3.0\sigma(I)$]	16 670	10 632
goodness-of-fit (S)	1.074	1.043
R_1 [$I > 2\sigma(I)$]	0.0271	0.0286
wR_2	0.0671	0.0750

X-ray Crystallographic Study. All measurements were carried out on a Rigaku Mercury CCD diffractometer at 193 K with graphite-monochromated Mo Kα ($\lambda = 0.71073$ Å) radiation. X-ray crystallographic data for compounds **2** and **3** were collected and processed using CrystalClear (Rigaku).[11] The structures were solved by direct methods using SHELXS-97,[12] and the refinements against all reflections of the compounds were performed using SHELXL-97.[13] All non-hydrogen atoms were refined anisotropically. The hydrogen atoms were positioned with idealized geometry and refined with fixed isotropic displacement parameters. Relevant crystal and collection data parameters and refinement results can be found in Table 1.

Results and Discussion

Theoretical Calculations. The molecular structures of DMT−TTF−py (**1**) and DMT−TTF−pyH$^+$ (**2**) were fully optimized using the B3LYP functional set and the 6-31G basis set.[9] Figure 1 displays the minimum energy structures afforded by the calculations. The structure of **1** is basically in accordance with that in the solid state observed from X-ray crystallographic study,[10] although there are some minor differences in specifics (bond distances and angles) between the calculated data and the experimental data. Figure 2 displays the atomic orbital population calculated for the HOMO and LUMO of **1** and **2**. For the HOMO of the compounds, the orbital is mainly located over the TTF moiety with small contributions of the pyridyl group, while for the LUMO, the orbital is mainly located on the pyridyl group. When the proton is added to the pyridyl group of **1**, it is apparent for DMT−TTF−pyH$^+$ that the pyridyl group is conjugated more efficiently with the dithiole ring that is directly bonded and the π-electron density shifts to the pyridyl group.

X-ray Crystal Structure of Compound 2. The protonated ion DMT−TTF−pyH$^+$ can be prepared by proton-transfer reactions from acids, such as adding *p*-methyl benzenesulfonic acid to **1**; however, crystals with good quality were obtained by reaction with acetylacetone in the presence of $Cu(NO_3)_2$ in a MeOH−CH_2Cl_2 mixed solvent. The crystal structure of DMT−TTF−py$^+$H·NO_3^- (Figure 3a) has been determined by X-ray crystal diffraction. The compound crystallizes in a monoclinic system with four chemical formulas in a unit cell. The cation of the molecule takes approximately a planar structure except two methyl groups. Two dithiole planes in the TTF unit have slight twisting with a dihedral angle of 6.0° with mean deviations of atoms from the planes of the five-member rings being 0.0091 and 0.0174 Å, respectively. The pyridyl group is conjugated completely with one dithiole ring that is directly bonded. The mean

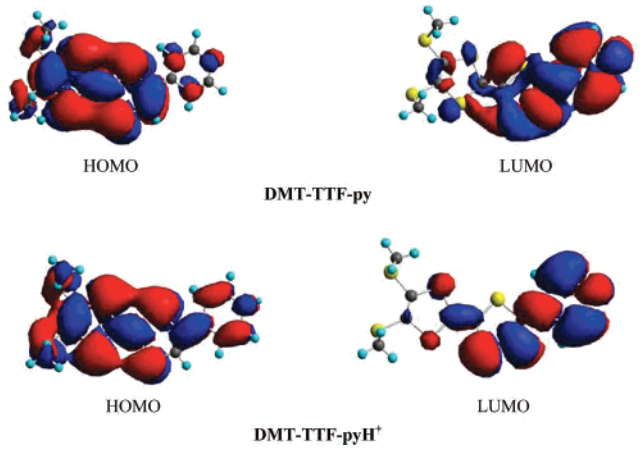

Figure 2. Calculated atomic orbital population for the HOMO and LUMO of DMT−TTF−py and DMT−TTF−pyH$^+$.

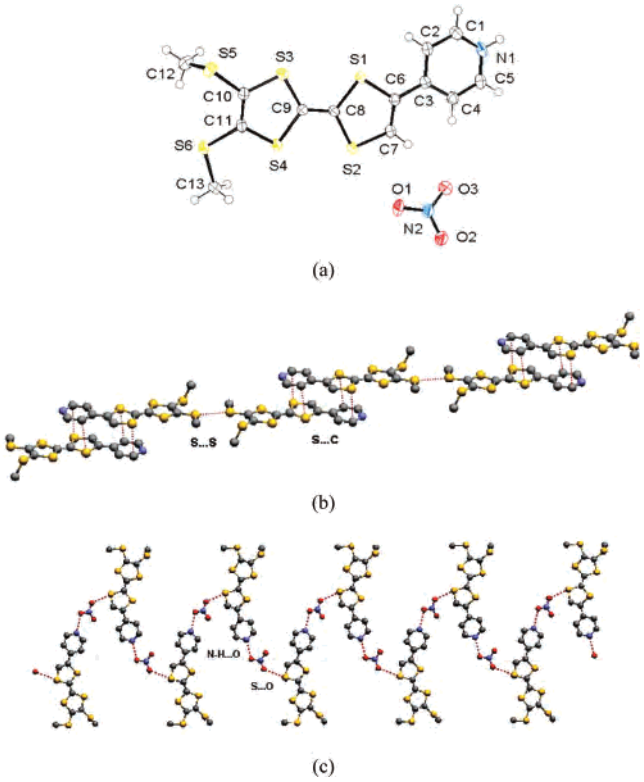

Figure 3. (a) ORTEP view of compound **2** with atomic-labeling scheme. (b) 1-D contact chain with short S···S and S···C contacts. (c) Interactions between the anion of NO_3^- and the cation.

(11) Rigaku Corp. 1999. CrystalClear Software User's Guide, Molecular Structure Corp: 2000. Pflugrath, J. W. *Acta Crystallor., Sect. D.* **1999**, *55*, 1718−1725.
(12) Sheldrick, G. M. *SHELXS-97, Program for structure solution*; Universität of Göttingen: Göttingen, Germany, 1999.
(13) Sheldrick, G. M. *SHELXL-97, Program for structure refinement*; Universität of Göttingen: Göttingen, Germany, 1997.

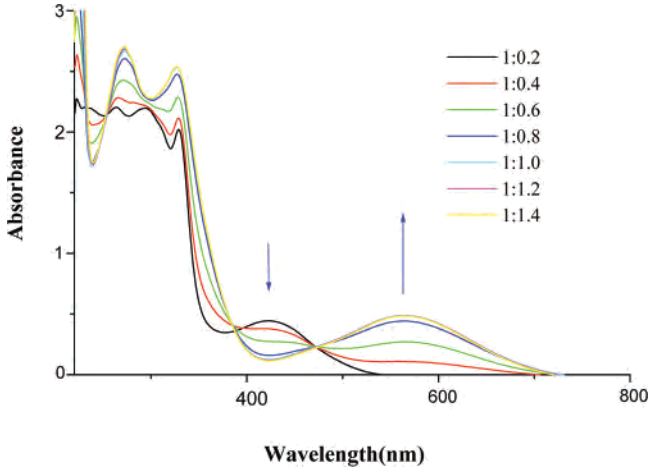

Figure 4. Absorption spectra of DMT−TTF−py (10^{-4} mol L^{-1}) in CH_2Cl_2/CH_3CN (in 1:1 volumes) with increasing concentration of *p*-methyl benzenesulfonic acid (molar ratio).

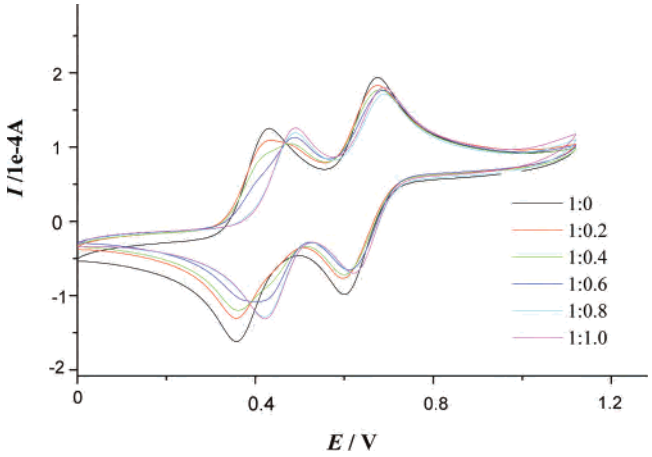

Figure 5. Cyclic voltammogram of DMT−TTF−py (10^{-3} mol L^{-1}) (CH_2Cl_2/CH_3CN in 1:1 volumes, Bu_4NClO_4, 0.1 mol L^{-1}, 100 mV s^{-1}) with increasing concentration of *p*-methyl benzenesulfonic acid.

deviation of the atoms from the plane of the pyridyl group is 0.0026 Å, and the dihedral angle between least-squares planes of the pyridyl group and the dithiole ring is 1.2°, while the dihedral angle for the non-protonated compound is 25.9°.[10] This result is in accordance with that of the calculation, namely, conjugation of the pyridyl group with the TTF plane is enhanced when the compound is protonated. In the solid state, the pyridyl−dithiole planes are face to face self-assembled to a dimeric structure with short S···C stacking (3.396 and 3.420 Å), which further contacts each other (S···S 3.206 Å, a very short contact), forming a 1-D chain (Figure 3b). The anion NO_3^- is linked to the cation by a N−H···O hydrogen bond (2.6935 Å) and a short S···O contact (3.133 Å) (Figure 3c). The hydrogen bond is a typical one with a H···O distance of 1.82 Å and N−H···O angle of 175.3°.

Intramolecular Charge Transfer (ICT) of Compound 2. The UV−vis spectra of DMT−TTF−py upon addition of *p*-methyl benzenesulfonic acid were measured, and the results are plotted in Figure 4. All measurements were carried out in a mixed solvent (CH_2Cl_2:CH_3CN, 1:1 in volume). The ligand shows a moderately intense absorption band at 425 nm, while such a band is absent for the parent TTF compound and is assigned to intramolecular charge transfer (photoexcited ICT).[2b,7e] The intensity of this band decreases monotonically with increasing acid concentration (*p*-methyl benzenesulfonic acid), which is accompanied by a new band at 566 nm appearing gradually. Since it has been established by theoretical calculation that the HOMO is located on the TTF moiety for compound DMT−TTF−py while the LUMO is located on the electron-acceptor fragment, the band change before and after addition of H^+ is attributed to alteration of the ICT excitation (HOMO → LUMO). The ICT band with a large red shift, $\Delta\lambda$ about 136 nm, indicates that the protonated pyridyl group is an efficient electron acceptor, which makes the ICT become easier. Thus, the protonated compound **2** is a good intramolecular D−A compound. The TTF materials with good D−A property are considered to be good candidates for molecular-scale electronic devices,[2b] such as a field-effect transistor and NLO materials. The bands at $\lambda < 370$ nm are assigned to the local transition in the TTF moiety.[7e]

The calculation demonstrated that the energy levels of the entire set of MOs dropped greatly because of protonation, especially the LUMO (see Supporting Information). Thus, a simultaneous reduction in the energy gap ΔE ($E_{LUMO} - E_{HOMO}$) happened, which results in the large red shift of the ICT absorption peak, $\Delta E_L = 3.529$ eV and $\Delta E_{HL+} = 1.445$ eV. Although the calculated data of the ICT bands deviate somewhat from the experimental data, due to theoretical calculations they are not considered to be effect of the solvents, the large red shift of the band is in agreement with that observed.

Corresponding electrochemical properties were measured and carried out in the same solvent as used for the UV−vis spectra measurement. Figure 5 presents changes of the potential of compound **1** upon addition of *p*-methyl benzenesulfonic acid. Two couples of reversible redox peaks are detected corresponding to the $TTF/TTF^{\bullet+}$ and $TTF^{\bullet+}/TTF^{2+}$ redox couples. $E_{1/2}(1)$ and $E_{1/2}(2)$ are 0.494 and 0.797 V vs SCE. When 0.2, 0.4, and 0.6 equiv of *p*-methyl benzenesulfonic acid is added to the solution, a new reversible redox wave appears at 0.571 V. Then on continually adding the acid, the original $E_{1/2}(1)$ wave completely disappears and only two pairs of reversible redox waves are displayed. Thus, the peaks of the first redox waves shift to higher potential with $\Delta E_{1/2}(1) = 0.077$ V. The large potential shift, about 80 mV to the positive side, is attributed to the decrease of the electron density on the TTF framework due to formation of the electron-withdrawing group $-pyH^+$. In view of the theoretical calculation, the positive shift of $E_{1/2}(1)$ of the protonated species is due to the large energy drop of the HOMO when the proton is added to **1**.

However, the second redox peaks are not significantly affected by addition of *p*-methyl benzenesulfonic acid. The equilibrium in this case is similar to the system of macrocyclic ethers with TTFs for redox recognition of alkali-metal ions.[3a] The proton is dissociated when the TTF moiety is two electron oxidized, and thus, oxidation-coupled ionization

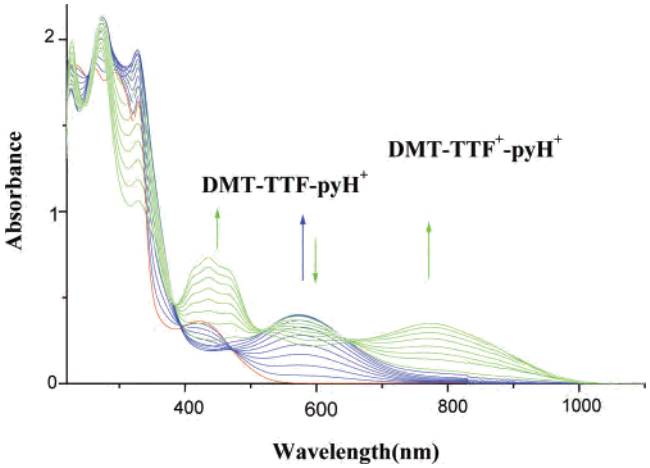

Figure 6. Absorption spectra of DMT−TTF−py (10^{-4} mol L^{-1}) in CH_2Cl_2/CH_3CN (in 1:1 volumes) with increasing concentration of $Fe(ClO_4)_3 \cdot 6H_2O$ (original compound **1**, red; first equilibrium, blue; second equilibrium, green).

Scheme 1

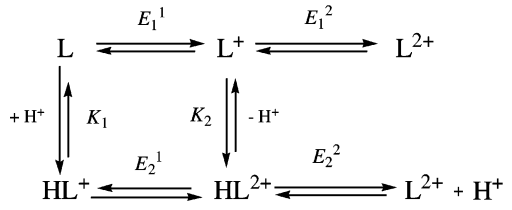

of proton occurs.[14] Proposed reactions of proton association/dissociation and oxidation/reduction of the TTF salt are described in Scheme 1, which might be used as a redox-controlled pH system.

Chemical Oxidation of Compound 1. Chemical oxidation of compound **1** in $CH_3CN-CH_2Cl_2$ mixed solvent was carried out by successive addition of $Fe(ClO_4)_3 \cdot 6H_2O$ as the oxidizing reagent (CAUTION: All metal perchlorates must be regarded as potentially explosive. Only a small amount of compound should be prepared, and it should be handled with caution). UV−vis spectra of the reaction system were recorded (Figure 6). At first addition of $Fe(ClO_4)_3 \cdot 6H_2O$ led to the disappearance of the band at 427 nm (ICT of the neutral DMT−TTF−py) and development of a new band at 570 nm. The change in spectra is completely in accordance with that found on addition of *p*-methyl benzenesulfonic acid (see Figure 4). Therefore, the first stage of the reaction is not an oxidation process but a protonation process due to hydrolysis of the Fe(III) ion. When continually adding $Fe(ClO_4)_3 \cdot 6H_2O$, new band at 772 nm appeared, which shows the characteristic band of the radical $TTF^{\bullet+}$ cation.[2b,7e] To confirm the conclusion, chemical oxidation in the same mixture of solvent was also carried out by successive addition of iodosobenzene diacetate as oxidizing reagent in the presence of *p*-methyl benzenesulfonic acid ($PhI(OAc)_2/C_7H_8SO_3$) (Supporting Information, Figure 1).[15] In that case chemical oxidation led to the same characteristic band of the cation radical (772 nm). On the basis of these experiment results, the reactions are summarized as in Scheme 2 and the species oxidized is protonated **1**.

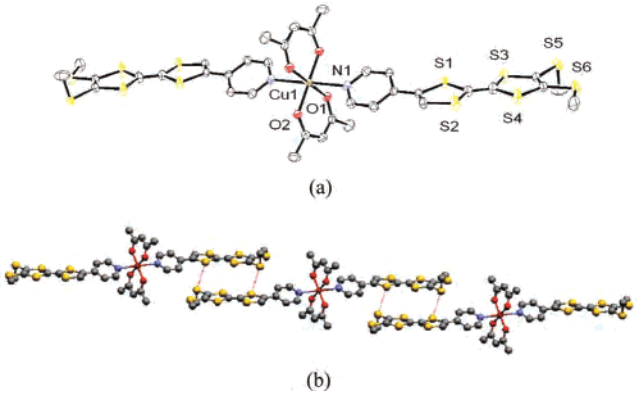

Figure 7. (a) ORTEP view of compound **3** with selected atomic-labeling scheme. (b) 1-D chain structure of compound **3** with short S···S contacts.

Scheme 2

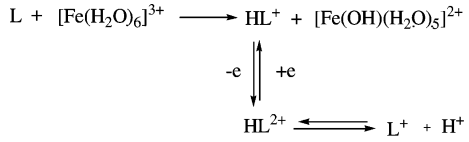

Coordination Ability of the Lone-Pair Electron in the Pyridyl Group. In the presence of acetylacetone (Hacac) and $Cu(NO_3)_2$ the pyridyl group acts as an acceptor for proton which is released from Hacac and the acac anion coordinates to Cu(II) ion at the same time (preparation of **2**). When $Cu(NO_3)_2$ is replaced by $Cu(OAc)_2$, the anion OAc^- can act as a proton acceptor. Then the TTF−py coordinates axially to the square-coordinated $Cu(acac)_2$, forming a new complex $Cu(acac)_2(DMT-TTF-py)_2$ (**3**). Because the pK_b data for OAc^- and py are very close and the pyridyl group is a good axial ligand, the pyridyl group prefers coordinating to Cu(II) in the presence of acetic anion. It is a good example of competitive reactions for coordination equilibrium and protonation equilibrium. The reactions are listed as follows

$$2\text{Hacac} + Cu^{2+} + 2\text{DMT}-\text{TTF}-\text{py} \rightarrow Cu(acac)_2 + 2(\text{DMT}-\text{TTF}-\text{pyH})^+$$

$$2\text{Hacac} + Cu(OAc)_2 + 2\text{DMT}-\text{TTF}-\text{py} \rightarrow Cu(acac)_2(\text{DMT}-\text{TTF}-\text{py})_2 + 2\text{HOAc}$$

The crystal structure of $Cu(acac)_2(DMT-TTF-py)_2$ has also been determined by X-ray crystal diffraction (Figure 7a). The compound crystallizes in a triclinic system with one chemical formula in a unit cell. The neutral molecule has an inverted center located at the metal ion. The TTF moiety takes approximately a planar structure except two methyl groups. However, unlike the protonated ligand, the pyridyl group is

(14) (a) Lin, H.-H.; Yan, Z.-M.; Dai, J.; Zhang, D.-Q.; Zuo, J.-L.; Zhu, Q.-Y.; Jia, D.-X. *New J. Chem.* **2005**, 509−513. (b) Zhu, Q.-Y.; Lin, H.-H.; Dai, J.; Bian, G.-Q.; Zhang, Y.; Lu, W. *New J. Chem.* **2006**, 1140−1144.

(15) (a) Giffard, M.; Mabon, G.; Leclair, E.; Mercier, N.; Allain, M.; Gorgues, A.; Molinie, P.; Neilands, O.; Krief, P.; Khodorkovsky, V. *J. Am. Chem. Soc.* **2001**, *123*, 3852−3853. (b) Gautier, N.; Samuel, R.; Süahin, Y.; Levillain, E.; Leroy-Lhez, S.; Hudhomme, P. *Org. Lett.* **2004**, *6*, 1569−1572.

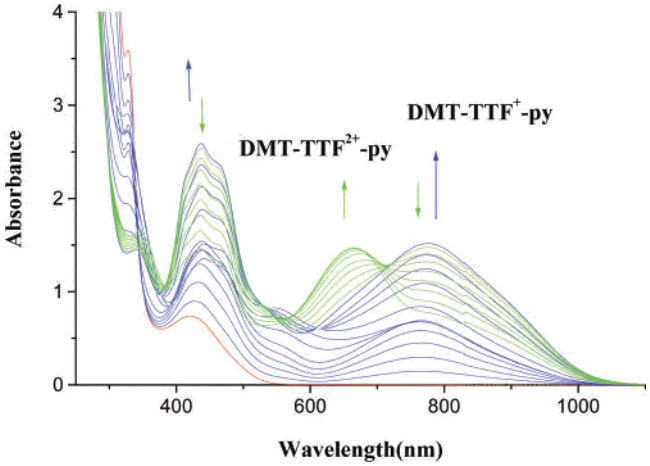

Figure 8. Absorption spectra of $Cu(acac)_2(DMT-TTF-py)_2$ (10^{-4} mol L^{-1}) in CH_2Cl_2/CH_3CN (in 1:1 volumes) with increasing concentration of $Fe(ClO_4)_3 \cdot 6H_2O$ (original complex, red; first oxidation, blue; second oxidation, green).

not well conjugated with the dithiole ring. The mean deviations from plane of the TTF moiety, except two methyl groups, and the plane of the pyridyl group are 0.0373 and 0.0040 Å, respectively. The dihedral angle between the least-squares planes of the TTF moiety and the pyridyl group is 26.3°, which is nearly the same as that of the free ligand **1**. The coordination sphere of the Cu ion takes an elongated octahedral geometry with two pyridyl groups of the ligands at the *z* direction and two acac anions at the *xy* plane. The TTF planes in the neighbor are face to face and self-assembly to a 1-D chain (Figure 7b) with short S···S contacts (3.528 Å).

Chemical Oxidation of Compound 3. Chemical oxidation of complex **3** was carried out, and the UV−vis spectra were recorded (Figure 8). As usually observed for TTF derivatives, addition of $Fe(ClO_4)_3 \cdot 6H_2O$ to a solution of **3** led to the appearance of the band at 777 nm, which shows oxidation of the neutral TTF unit into the corresponding $TTF^{\bullet+}$ radical cation. The absorption intensity at 777 nm increased with increasing amounts of $Fe(ClO_4)_3 \cdot 6H_2O$ to about a 2 mol ratio of $Fe(ClO_4)_3 \cdot 6H_2O$ vs **3**; then the absorption intensity gradually declined when continually adding $Fe(ClO_4)_3 \cdot 6H_2O$. Concomitantly, a new absorption at about 664 nm appeared and the intensity increased gradually, which shows that some cation radicals $TTF^{\bullet+}$ have been oxidized further to dication TTF^{2+}.[4d,16] The appearance of an isosbestic point in this stage reveals that there is a two-species equilibrium about the TTF moiety in solution, cation radical $TTF^{\bullet+}$ and dication TTF^{2+}. A small peak appears at about 560 nm for the first oxidation step, which might be caused by the partial acidifying of compound **1** (see Figure 4). The change in the spectra of **3** is different from that of protonated **1** (Figure 6), which is only oxidized to cation radical $TTF^{\bullet+}$ by $Fe(ClO_4)_3 \cdot 6H_2O$ even in an excess amount of Fe(III) salt. The difference between protonated **1** and **3** in the absorption spectra means that the oxidation potential of the TTF moiety decreased when forming a complex with ligand **1**. The result can be explained by the CV measurements. Compound **3** exhibits two reversible one-electron redox waves, $E_{1/2}(1) = 0.475$ V and $E_{1/2}(2) = 0.777$ V, respectively, in the mixed solvent with $\Delta E_{1/2} = \sim 30$ mV, $E_{1/2}(2) - E_{1/2}(1)$ (Supporting Information Figure 3). The two peaks of the oxidation/reduction waves shift to lower potentials compared with the free ligand no matter what the acidity is. The down-shift of the potentials is due to the back-donating of the electron density from the neutral $Cu(acac)_2$ moiety.

(16) (a) Gomar-Nadal, E.; Veciana, L.; Rovira, C.; Amabilino, D. B. *Adv. Mater*. **1999**, *17*, 2095−2098. (b) Spang-gaard, H.; Prehn, J.; Nielsen, M. B.; Levillain, E.; Allain, M.; Becher, J. *J. Am. Chem. Soc*. **2000**, *122*, 9486−9494.

Conclusion

A new protonated bifunctional pyridine-based TTF derivative and a copper(II) complex have been studied. The electronic spectra and theoretical calculation show that an intramolecular charge transfer exists between the TTF moiety and the pyridyl group and the pyridium substituent is the strongest π-electron acceptor. Compared with other TTF−pyridine-based systems, this nonspacer compound has the largest ICT effect (UV−vis, $\Delta\lambda$ =136 nm; CV, $\Delta E_{1/2}(1) =$ 77 mV). The materials having a large ICT effect are considered as good candidates for molecular-scale electronic devices and NLO devices. It is also noteworthy that the TTF moiety could be oxidized to dication by $Fe(ClO_4)_3 \cdot 6H_2O$ when forming a complex, while the protonated ligand can only be oxidized to the monocation radical by $Fe(ClO_4)_3 \cdot 6H_2O$ even in an excess amount of Fe(III) salt, which can be used to control the oxidation process to obtain neutral TTF, cation radical $TTF^{\bullet+}$, or dication TTF^{2+}. Crystal structures of the protonated compound and complex have been obtained. The dihedral angle between least-squares planes of the pyridyl group and the dithiole ring might reflect the intensity of the ICT effect.

Acknowledgment. This work was supported by the National NSF (20371033) and the NSF of the Education Committee of Jiangsu Province (grant 06KJB150102)

Supporting Information Available: Crystallographic data of **2** and **3** in CIF format. This material is available free of charge via the Internet at http://pubs.acs.org.

IC700672E